DOI: http://dx.doi.org/10.12989/cac.2012.10.3.241

Flexural behavior model for post-tensioned concrete members with unbonded tendons

Kang Su Kim and Deuck Hang Lee*

Department of Architectural Engineering, University of Seoul, Seoul, Korea

(Received April 11, 2011, Revised January 19, 2012, Accepted March 19, 2012)

Abstract. The need for long-span members increases gradually in recent years, which makes issues not only on ultimate strength but also on excessive deflection of horizontal members important. In building structures, the post-tension methods with unbonded tendons are often used for long-span members to solve deflection problems. Previous studies on prestressed flexural members with unbonded tendons, however, were mostly focused on the ultimate strength. For this reason, their approaches are either impossible or very difficult to be implemented for serviceability check such as deflection, tendons stress, etc. Therefore, this study proposed a flexural behavior model for post-tensioned members with unbonded tendons that can predict the initial behavior, before and after cracking, service load behavior and ultimate strength. The applicability and accuracy of the proposed model were also verified by comparing with various types of test results including internally and externally post-tensioned members, a wide range of reinforcement ratios and different loading patterns. The comparison showed that the proposed model very accurately estimated both the flexural behavior and strength for these members. Particularly, the proposed model well reflected the effect of various loading patterns, and also provided good estimation on the flexural behavior of excessively reinforced members that could often occur during reinforcing work.

Keywords: unbonded tendon; prestress; flexural behavior; post-tension; flexural strength.

1. Introduction

Unlike the prestressed concrete members with bonded tendons, the strain compatibility condition between concrete and tendons at a section cannot be utilized in the analysis of the prestressed concrete members with unbonded tendons due to the unbonded behavior between concrete and tendon. This makes it difficult to predict the flexural strength of unbonded post-tensioned concrete members (hereinafter, "UPT"), which has thus been an important research subject for many researchers. Our understanding on this issue, however, is still very limited, and the code equations (AASHTO-LRFD 2004, 2007, ACI Committee 318 2005, 2008, BSI 8110-85 1985, CAN-A23.3-M94 1994, DIN 4227 1980, KCI-M-07 2007, NEN 3880 1984) and many existing approaches (Lee and Kim 2011, Lee *et al*. 2010, Zhou and Zheng 2010, Au *et al*. 2009, Du *et al.* 2008, Ozkul *et al.* 2008, Tan and Tjandra 2007, Bui and Niwa 2006, Harajli 2006, Sivaleepunth *et al.* 2006, Ozkul *et al.* 2005, Roberts-Wollmann *et al.* 2005, Au and Du 2004, Ng 2003, Moon *et al.* 2002, Allouche *et al.* 1999(a), 1999(b), Harali *et al*. 1999, Lee *et al.* 1999, Lim *et al.* 1999, Harajli and Kanj 1991, 1997, Chakrabarti 1995, Campbell and Chouinard 1991, Naaman and Alkhairi 1991(a), 1991(b), Tan and Ng 1991, Harajli 1990, MacGregor *et al.* 1989, Du and Tao 1985, Mojtahedi and Gamble 1978,

* Corresponding author, Ph. D. Candidate, E-mail: dklee@uos.ac.kr

Tam and Pannell 1976, Bondy 1970, Janney *et al.* 1956, Warwaruk *et al.* 1962), proposed for the design of the ultimate strength of UPT members, yield very different results and often inaccurate predictions. Therefore, authors, in their former research (Lee and Kim 2011), revised the existing approaches (MacGregor *et al.* 1989, Harajli 1990, 2006, Au and Du 2004, Roberts-Wollmann *et al.* 2005, Bui and Niwa 2006, Ozkul *et al.* 2008) on the flexural strength of UPT members, and proposed an ultimate strength prediction method that considers key factors such as loading patterns and reinforcement ratios. They also verified the rationality and accuracy of the proposed approach comparing to the 177 test results collected from previous studies (Janney *et al.* 1956, Warwaruk *et al.* 1962, Du and Tao 1985, Harajli and Kanj 1991, Campbell and Chouinard 1995, Chakrabarti 1995, Moon *et al.* 2002, Ozkul *et al.* 2008).

On the other hand, the flexural behavior under service load is also very important when unbonded post-tension method is applied, because often the UPT members are used for deflection control rather than strength enhancement. Previous studies (Janney *et al.* 1956, Warwaruk *et al.* 1962, Bondy 1970, Tam and Pannell 1976, Mojtahedi and Gamble 1978, Du and Tao 1985, MacGregor *et al.* 1989, Harajli 1990, 2006, Harajli and Kanj 1991, Naaman and Alkhairi 1991a, 1991b, Campbell and Chouinard 1995, Chakrabarti 1995, Allouche *et al.* 1999a, 1999b, Lee *et al.* 1999, Au and Du 2004, Roberts-Wollmann *et al.* 2005, Bui and Niwa 2006), however, mainly focused on the ultimate strength of UPT members, by which it is either impossible or very difficult to examine serviceability of UPT members.

Therefore, this study, which comes after the proposal of an approach for the prediction of the flexural strength of UPT members[39], aims to propose a flexural behavior model that can predict the behavior before and after cracking, under service load state and ultimate strength of UPT members as well. It also aims to verify the applicability and accuracy of the proposed model by comparing the predicted values to experimental test results reported in literatures (Janney *et al.* 1956, Warwaruk *et al.* 1962, Du and Tao 1985, Harajli and Kanj 1991, Campbell and Chouinard 1995, Chakrabarti 1995, Moon *et al.* 2002, Ozkul *et al.* 2008).

2. Research significance

While most previous studies concentrated on the ultimate strength of UPT members, this study proposed a flexural behavior model that can predict the flexural behavior of UPT members under service load as well as ultimate strength. The applicability and accuracy of the proposed model are also verified with test data. Particularly, the proposed model well reflected the effect of various loading patterns, and provided very good estimation of flexural behavior for over-reinforced members that can often occur during onsite work for strength enhancement.

3. Previous research

3.1 Ultimate strength of unbonded tendons

To investigate the flexural strength of UPT members, Warwaruk *et al.* (1962) performed an experimental study with the primary test variables of the amount of bonded reinforcing steel and the moment distribution shape. Based on their results, they proposed an approximate equation for ultimate tendon stresses introducing the coefficients to account for the effect of bonded reinforcing steel and loading patterns. Harajli (1990) proposed the concept of idealized equivalent plastic hinge length, based on which Bui and Niwa (2006) and Lee *et al.* (1999) performed a regression analysis of ultimate tendon stresses (f_{ps}). MacGregor *et al.* (1989) presented the rigid body model, wherein all strains are concentrated on the plastic hinge, and later, Roberts-Wollmann *et al.* (2005) and Harajli (2006) also complemented this model. Naaman *et al.* (1991a, 1991b) proposed a design equation that considers not only the sectional properties but also the tendon profile and loading patterns as well as the moment-curvature relationship in the longitudinal direction of a member. They also empirically determined the bond coefficient that is a key concept in their approach.

In many previous studies (MacGregor *et al.* 1989, Harajli 1990, Au and Du 2004, Roberts-Wollmann *et al.* 2005, Bui and Niwa 2006, Harajli 2006, Ozkul *et al.* 2008), the length of plastic hinge plays a key role in calculating the total amount of deformation of unbonded tendons (ΔL). It is very difficult, however, to accurately predict the length of plastic hinge, which is considered to be a primary reason for errors in estimating the stress increase in unbonded tendons (Δf_{ps}). Therefore, authors, in their previous research (Lee and Kim 2011), used the assumption that the deformation is concentrated on the maximum moment zone at ultimate, based on the test results of Warwaruk *et al.* (1962) and Campbell and Chouinard (1991), and proposed a flexural strength model for UPT members. The ultimate stress (f_{ps}) and the ultimate strain (ε_{ps}) of unbonded tendons in their proposed strength model are

$$f_{ps} = f_{pe} + \Delta f_{ps} \le f_{py} \tag{1a}$$

$$\varepsilon_{ps} = \varepsilon_{pe} + \Delta\varepsilon_{ps} \tag{1b}$$

where f_{pe} and ε_{pe} are effective prestress and prestrain in tendons, respectively, f_{py} and ε_{py} are yield stress and yield strain of tendon, respectively, and Δf_{ps} refers to the additional stress in tendons at ultimate, which corresponds to the additional strain of tendon ($\Delta\varepsilon_{ps}$) at ultimate

$$\Delta\varepsilon_{ps} = \alpha k \frac{\varepsilon_{cu}}{c_m}(d_p - c_m) \tag{2}$$

where α, k, ε_{cu}, d_p and c_m refer to the coefficient of the moment distribution shape (See Table 1), the ratio of the maximum moment zone length to the member length, the ultimate compressive strain of concrete, the distance from the extreme top fiber to the centroid of tendons, and the neutral axis depth at the maximum moment zone, respectively, which is

$$c_m = \frac{-B \pm \sqrt{B^2 - 4AC}}{2A} \tag{3a}$$

and, A, B and C are

$$A = 0.85 f_c' b \beta_1 \tag{3b}$$

$$B = -(f_s A_s - f_s' A_s' - k\varepsilon_{cu} E_p A_{ps} + \varepsilon_{pe} E_p A_{ps}) \tag{3c}$$

Table 1 Coefficients of moment distribution shape (α) for different loading patterns

Loading pattern	1 point loading	uniform loading	2 point loading
α	0.75	1.0	1.0

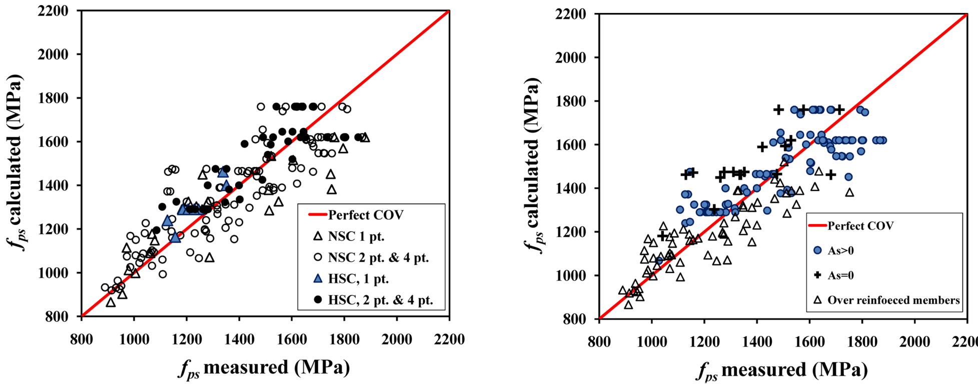

(a) Effect of loading patterns and concrete strength (b) Effect of bonded reinforcement and over-reinforcement

Fig. 1 Comparison of ultimate unbonded tendon stresses (f_{ps}) calculated by the proposed strength model and test results

$$C = -k\varepsilon_{cu}E_pA_{ps}d_p \tag{3d}$$

In Eq. (3), A_{ps}, A_s and A_s', refer to the area of unbonded tendons, reinforcing bars in tension and compression, respectively, and E_p is the elastic modulus of the tendon.

Fig. 1 compares the flexural strength obtained from the proposed method and the test results of 177 UPT members that were tested under different loading patterns and have various amount of bonded reinforcing steel, including those not having bonded reinforcing bars. It demonstrates that the predicted strength by the proposed method well matches the test results regardless of the different characteristics of test specimens. Particularly, the proposed model predicts very well the strength of over-reinforced members, which can happen during repairs or retrofit works, and of high-strength members that are widely used. The detailed information on the derivation of the proposed strength model and the analysis of various approaches can be found in the References (Lee and Kim 2011).

3.2 Flexural behavior model

While many studies have been conducted to estimate the flexural strength of UPT members, there are only a few studies on flexural behavior models for these members. Lee *et al.* (2010) proposed the simple summation model, shown in Fig. 2(a), which analyzes the tendon forces considering the

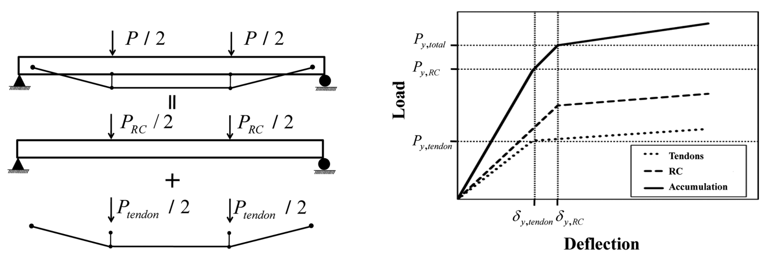

(a) Summation of two member systems (b) Simple summation model

Fig. 2 Description of simple summation model (Lee *et al.* 2010)

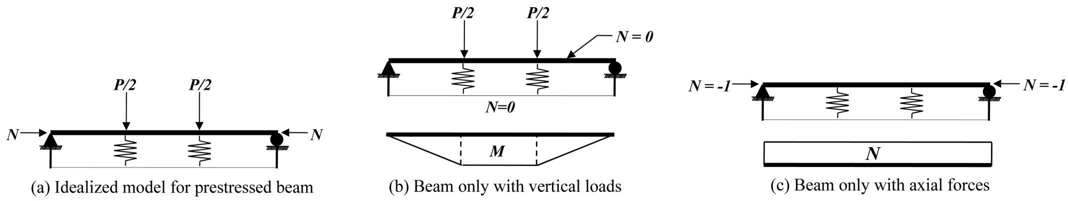

Fig. 3 Unit load trussed-beam model (Ozkul *et al.* 2005)

unbonded tendons as simple tension members with an assumption that the deflections of tendons and concrete are identical at drape points. As Fig. 2(b) shows, the resisting forces of reinforced concrete and tendons are simply summated to get the total member force. While this process seems to be simple, the analysis error becomes larger after cracking, because there is a big difference in inelastic behavior of concrete member between the concrete member alone and the concrete member with tendons. It is also not applicable in case loading points and drape points are different, or straight or curved tendons are used. Moon *et al.* (2002) also proposed a flexural behavior model. This model is ultimately based, however, on the ultimate tendon stress prediction equation from the regression analysis, and therefore, it is believed to be somewhat unreasonable to use this model to predict flexural behavior of UPT members. Tan and Ng (1991) proposed an equation based on the secondary moment effect, which occurs additionally due to change of the eccentricity of tendons in the location of the anchorage device for externally post-tensioned members. On the other hand, Ozkul *et al.* (2005) used the idealized trussed-beam model shown in Fig. 3, and applied the principles of virtual work by dividing the loading system into two: a system subjected to two-point loading without prestressing forces (Fig. 3(b)) and another one with prestressing axial force only (Fig. 3(c)). This model can predict the unbonded tendon stress and the flexural behavior of UPT members considering effect moment of inertia before and after cracking, but it tends to underestimate the flexural stiffness of members (Ozkul *et al.* 2005).

Recently, Ozkul *et al.* (2008), along with Harajli, revised the idealized trussed-beam model and proposed the general incremental analysis (GIA). GIA divides the loading stages into the linear elastic state, the cracking state and the ultimate state, and calculates the load-displacement relationship, which results in a relatively accurate analysis. This model, however, utilized the strength model with the plastic hinge length at ultimate state to predict the flexural behavior under service load, which seems to be unreasonable. In addition, this model does not consider the effect of the loading patterns on the flexural behavior.

4. Proposed flexural behavior model of UPT members

Before flexural cracking, the curvature distribution in the longitudinal direction is identical to the pattern of the flexural moment, where all sections of the concrete including tension side contribute to the flexural strength. After the flexural crack occurs within the maximum moment region of the member as the loading increases, the curvature increases locally in the cracked region, as Fig. 4(a) shows, which is different from the pattern of the flexural moment. Since it is very difficult to get a precise estimation of such a change in the curvature distribution, researchers have assumed that the curvature would be concentrated within the equivalent plastic hinge length and have proposed flexural behavior (or strength) models. (Harajli 1990, Lee *et al.* 1999, Ozkul *et al.* 2008) The rigid-

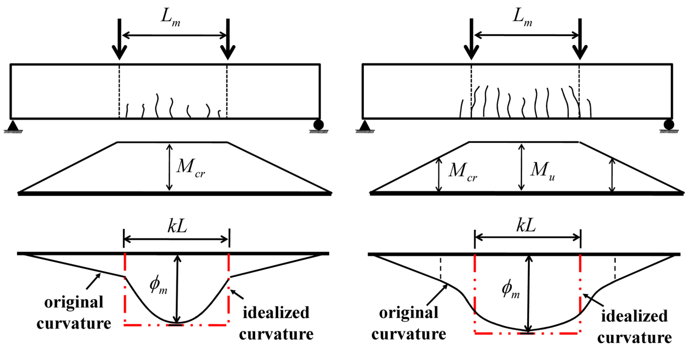

(a) Cracking load stage $P_a \approx P_{cr}$ (b) Ultimate load stage $P_a \approx P_u$

Fig. 4 Bending moment and curvature distribution at different loading stages

body model (MacGregor *et al.* 1989, Roberts-Wollmann *et al.* 2005, Bui and Niwa 2006, Harajli 2006) proposed later also considered that the equivalent plastic hinge length at ultimate state is a very important factor in predicting the flexural behavior of UPT members. All the existing models that utilize the concept of equivalent plastic hinge length, however, are based on the ultimate state, which is considered that these models are not suitable for flexural behavior models. Furthermore, it is very difficult to predict the plastic hinge length itself, and consequently, there are huge differences on the plastic hinge lengths among researchers.

Therefore, in this study as shown in Figs. 4(a) and (b), the maximum curvature distribution has been idealized by simplifying the curvature within the maximum moment zone, based on the observation on the test results of Warwaruk *et al.* (1962). As explained in the previous study (Lee and Kim 2011), in the case of the member with the minimum bonded reinforcing steel specified in codes of practice, the measurement of the strain of the extreme top compression fiber from the service load stage to the ultimate stage shows that the deformation is concentrated approximately within the maximum moment region. And even when there is no bonded reinforcing steel, a few cracks under the two-point loading can be adequately developed within the maximum moment zone. (Janney *et al.* 1956, Warwaruk *et al.* 1962, Campbell and Chouinard 1991) In this study, the flexural strength model, proposed in the authors' previous research (Lee and Kim 2011), has been extended to develop a flexural behavior model for UPT members, based on the assumption of the idealized curvature distribution at the maximum moment zone. In addition, the compatibility condition of UPT members, in which the total amount of elongation in the tendon length between anchorages shall be identical to the total amount of the deformation in the concrete at the level of tendon, has been applied.

4.1 Description of the flexural behavior model for UPT members

As described above, the flexural behavior model proposed in this study, extended from the strength model proposed in the authors' previous research (Lee and Kim 2011), utilizes the idealized curvature distribution at the maximum moment zone as shown in Fig. 4. Fig. 5(a) shows the stress-strain relationships of materials that were applied to the flexural behavior model. In the case of reinforcing steel, this study assumed a general elastic-plastic model to simplify the calculation and used the Ramberg-Osgood formula (Mattock 1979, Chen 1982) for the tendons. In the case of concrete, this study implemented the constitutive model proposed by Collins and Mitchell (1991), which can efficiently express nonlinear behavior, and wherein the stress (f_c) to strain (ε_c) relationships of concrete is expressed as

$$f_c = f_{ck}\left[2\left(\frac{\varepsilon_c}{\varepsilon_c'}\right) - \left(\frac{\varepsilon_c}{\varepsilon_c'}\right)^2\right] \tag{4}$$

where f_{ck} and ε_c' refer to the compressive strength of concrete and the corresponding strain, respectively. As Fig. 5(b) shows, the sum of the compressive force of concrete at a particular loading state can be determined from the integration of the concrete stress (f_c) that is distributed from the extreme compressive fiber of the section to the neutral axis (c), which is

$$\int_0^c f_c b dy = \alpha_1 f_{ck} \beta_1 cb \tag{5}$$

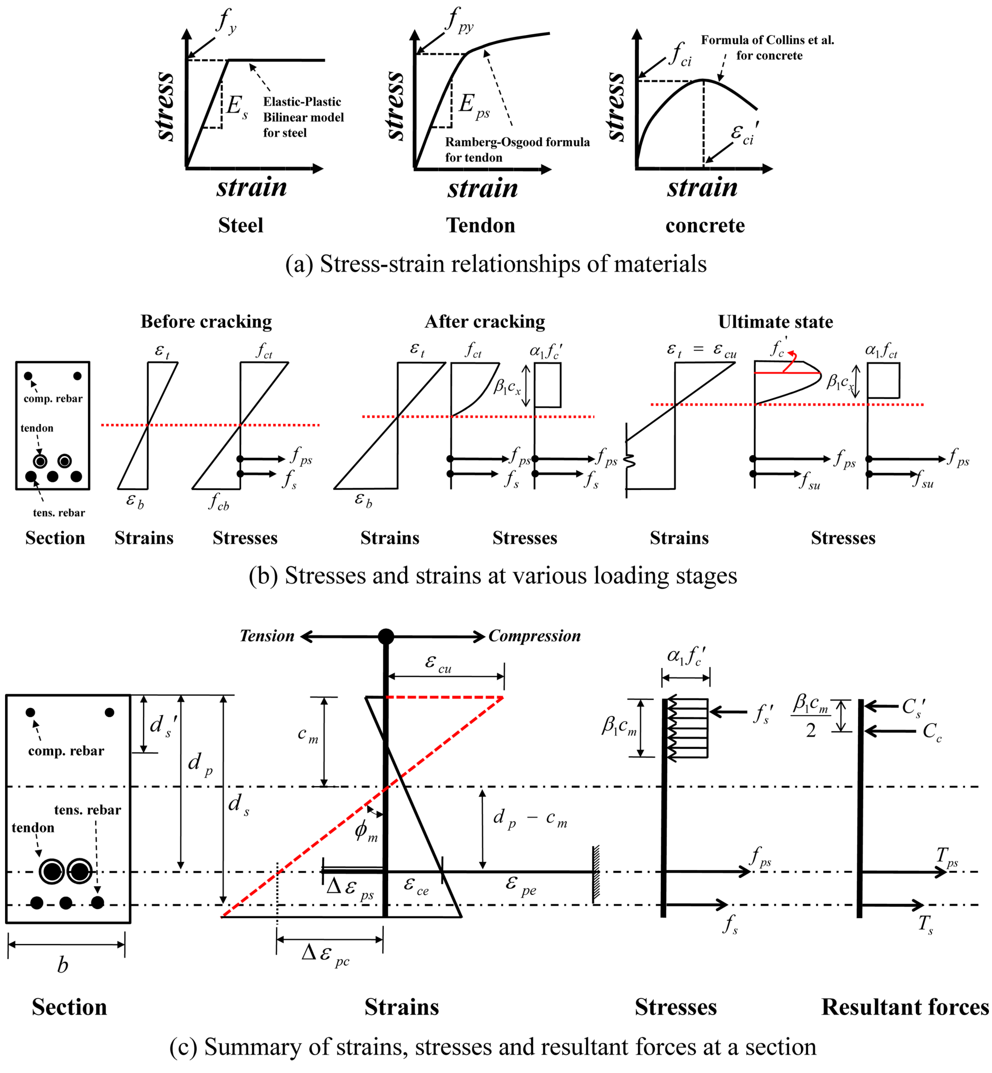

Fig. 5 Description of the proposed model

where b, c and y are the member width, the neutral axis depth from extreme fiber, and the vertical distance from a particular depth of the section to the neutral axis, respectively, and α_1 and β_1 are the width and depth factors of equivalent rectangular compressive stress block, respectively. From Eqs. (4) and (5), $\alpha_1\beta_1$ becomes

$$\alpha_1\beta_1 = \left(\frac{\varepsilon_t}{\varepsilon_c'}\right) - \frac{1}{3}\left(\frac{\varepsilon_t}{\varepsilon_c'}\right)^2 \tag{6}$$

where ε_t is the compressive strain of the extreme top fiber. Also, the distance from the neutral axis to the resultant force of the compressive stresses ($\bar{y}$) is

$$\bar{y} = \frac{\int_0^c f_c b\, y\, dy}{\int_0^c f_c b\, dy} = c - 0.5\beta_1 c \tag{7}$$

Therefore, from Eqs. (5), (6) and (7), the depth ratio of equivalent rectangular compressive stress block and neutral axis (β_1) is

$$\beta_1 = \frac{4 - \varepsilon_t/\varepsilon_{cu}}{6 - 2\varepsilon_t/\varepsilon_{cu}} \tag{8}$$

Then, the stress block factor (α_1) can be calculated by substituting Eq. (8) into Eq. (6).

If the strain of the extreme top fiber (ε_t) at an arbitrary loading stage is assumed to be as shown in Fig. 5(b), the strain at the location with a distance y from the neutral axis can be expressed by the assumed ε_t. In other words, strain (ε_x) at a certain location (y) can be expressed as

$$\varepsilon_x = \varepsilon_t + \frac{\varepsilon_b - \varepsilon_t}{h} y \tag{9}$$

where, h is the member height, and as Fig. 5(c) shows, ε_b is the strain at the extreme bottom fiber. While the value of ε_b also should be assumed in the initial calculation, the only one value of ε_b satisfies the equilibrium expressed in Eq. (14) with regard to the assumed ε_t; and therefore, the correct solution can be obtained from the iterative calculations. Once the strain of the extreme top and bottom fiber of the section (ε_t and ε_b) are determined, they can be used to calculate the neutral axis depth (c_x) and the strain of reinforcement. As shown in Fig. 5(b), before the cracking, i.e., until the strain of the extreme bottom fiber (ε_b) exceeds the cracking strain (ε_{cr}), the tensile stress of concrete below the neutral axis should be also included in the calculation of equilibrium. Here, the cracking strain (ε_{cr}) is

$$\varepsilon_{cr} = \frac{M_{cr}}{E_c I_g} y_b \tag{10}$$

where E_c, I_g and M_{cr} refer to the elastic modulus of concrete, the moment of inertia of the gross section, and the moment strength at which the tensile stress at the extreme bottom fiber reaches the cracking stress (modulus of rupture, f_r), respectively. For the value of f_r, $0.63\sqrt{f_c'}$ (ACI Committee 318 2005, 2008) has been used. If the strain of the extreme bottom tensile fiber of section exceeds the cracking strain (ε_{cr}), the tension force at the concrete below the neutral axis would be negligible and was ignored for simple calculation. The strains of tensile and compressive reinforcing steels (ε_s and ε_s') can be calculated by substituting the distance from the extreme top fiber of section to the centroid of tensile and compressive reinforcing steels (d and d') into Eq. (9), as follows

$$\varepsilon_s(\text{or } \varepsilon_s') = \varepsilon_t + \frac{\varepsilon_b - \varepsilon_t}{h} d(\text{or } d') \tag{11}$$

The stress of the reinforcing steel is calculated by substituting ε_s and ε_s' into the stress-strain relation curve of the reinforcing steel, as Fig. 5(a) shows. As expressed above, however, if the strain of the reinforcing steel (ε_s) exceeds the yield strain of steel (ε_y), the stress of the reinforcing steel (f_s) should be limited to the yield strength of steel (f_y). In other words

$$\text{If } \varepsilon_s < \varepsilon_y, \text{ then } f_s = E_s \varepsilon_s \tag{12a}$$

$$\text{If } \varepsilon_s \geq \varepsilon_y, \text{ then } f_s = f_y \tag{12b}$$

where E_s refers to the elastic modulus of reinforcing steel. The strain of tendons can be calculated by adding the additional strain [$\Delta\varepsilon_{ps}$, refer to Eq. (5)] to the effective prestrain (ε_{pe}), that is

$$\varepsilon_{ps} = \varepsilon_{pe} + \Delta\varepsilon_{ps} = \varepsilon_{pe} + \alpha k \frac{\varepsilon_t}{c_x}(d_p - c_x) \tag{13}$$

Then, the stress of the tendons corresponding to the strain was calculated from the Ramberg-Osgood formula.

Based on the section sectional resultant forces shown in Fig. 5(c), the equilibrium equation can be established as

$$\alpha_1 f_c' b \beta_1 c_x + f_s' A_s' - f_{ps} A_{ps} - f_s A_s = 0 \tag{14}$$

and the moment strength can be calculated by multiplying the distance from the location of the neutral axis that satisfies Eq. (14) to each sectional force, as follows

$$\begin{aligned} M_n &= C_c\left(c_x - \frac{\beta_1 c_x}{2}\right) + C_s(c_x - d_s') + \sum T(d - c_x) \\ &= \alpha_1 f_c' b \beta_1 c_x\left(c_x - \frac{\beta_1 c_x}{2}\right) + f_s' A_s'(c_x - d_s') + f_{ps} A_{ps}(d_p - c_x) - f_s A_s(d - c_x) \end{aligned} \tag{15}$$

From Fig. 5(c), the curvature in maximum moment region (ϕ_m) is also expressed as

$$\phi_m = \frac{\varepsilon_t}{c_x} = \frac{\varepsilon_b}{(h - c_x)} \tag{16}$$

By calculating the curvature and moment while increasing the aforementioned calculation procedures until ε_t reaches ε_{cu}, the moment-curvature relationship can be calculated at all loading stages. The calculation procedures of the proposed analysis model are shown in Fig. 6 as a flowchart.

5. Verification of the proposed method

To verify the proposed flexural behavior model, as shown in Figs. 7 and 8, the test results obtained from previous studies (Du and Tao 1985, Tan and Ng 1991, Lim *et al.* 1999, Moon *et al.* 2002) have been compared to analysis results. Table 2 shows the detailed properties of specimens,

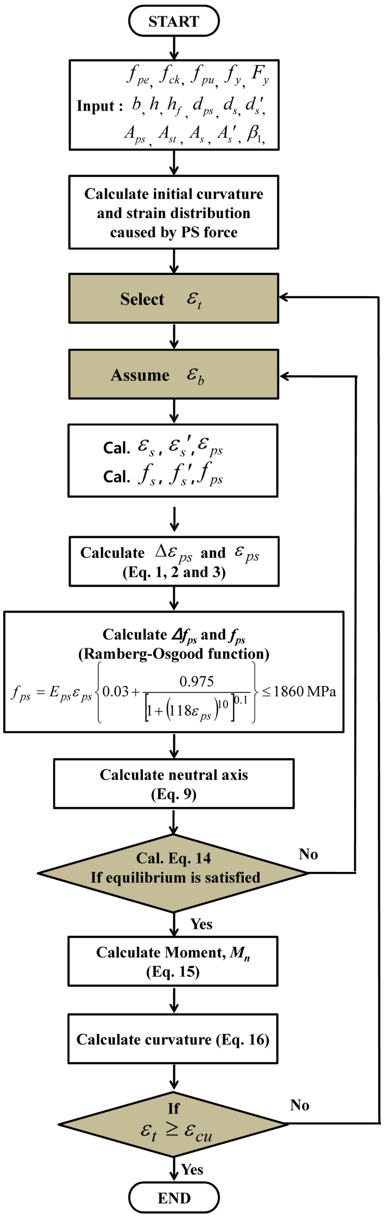

Fig. 6 Flow chart for calculation of the moment-curvature curve by the proposed model

including material strengths, amount of reinforcement and loading patterns.

5.1 Members under two-point loading

Figs. 7(a) to (e) show the specimens with rectangular section subjected to two-point loading. The specimens had various amounts of tendons and bonded reinforcing steels. Specimen A-2 in Fig. 7(a) had 0.45% of reinforcing steel ratio and 0.28% of the ratio of prestressing tendons, which

Table 2 Sectional properties of specimens

Specimen	$b(b_w)$ (mm)	h	f_c'	f_y (MPa)	f_{py}	f_{pu}	A_s (mm)	A_{ps}
				2 point loading				
A-2	160	280	30.6	430	1465	1790	157.0	98.0
A-5	160	280	30.6	400	1465	1790	308.0	78.3
A-7	160	280	30.6	400	1465	1790	308.0	39.2
A-3	160	280	30.6	430	1465	1790	236.0	156.8
A-9	160	280	33.1	395	1465	1790	804.0	156.8
F-1	200	300	23.5	420	1620	1860	135.5	118.9
				1 or 4 point loading				
F-2	200	300	23.5	420	1620	1860	135.5	118.9
J-1	200	350	23.5	420	1620	1860	253.0	39.6
B-2	160	280	30.6	430	1465	1790	157.0	98.0
T-1	300 (110)	300	30.0	530	1710	1860	397.0	109.6

corresponds to 0.23 of reinforcement index (R), where R is defined as follows (ACI Committee 318 2005, Korea Concrete Institute 2007)

$$R = \omega_p + \frac{d}{d_p}(\omega_s + \omega_s') \qquad \omega_p = \rho_p\frac{f_{pu}}{f_c'},\ \omega_s = \rho_s\frac{f_y}{f_c'},\ \omega_s' = \rho_s'\frac{f_y'}{f_c'} \tag{17}$$

where ρ_p, ρ_s and ρ_s' are the area ratio of tendon, tensile reinforcing steel and compressive reinforcing steel, and f_{pu}, f_y and f_y' are the tensile strength of tendon and the yield strengths of tensile and compressive reinforcing steels, respectively. Fig. 7(a) shows that the proposed model perfectly estimated the initial flexural stiffness of specimen A-2 before the cracking and also well predicted the member behavior after cracking including ultimate strength and near yielding moment.

Figs. 7(b) and (c) show specimens A-5 and A-7, which both had 0.88% reinforcing steel, but their prestressing steel ratios were 0.22% and 0.11%, respectively. The amount of bonded reinforcing steel in these two specimens was twice as much as in specimen A-2 in Fig. 7(a), and the amount of tendons in these specimens were about 2/3 and 1/3 of specimen A-2, respectively. The proposed model very accurately predicted the flexural behavior of these specimens wherein the amount of bonded reinforcing steel was greater than the amount of tendons. This shows that the proposed model reflects well the effect of the bonded reinforcing steel with respect to the change in the neutral axis, and also implies that the simplified curvature assumed in the proposed model applies quite well without much difficulty. Fig. 7(d) shows specimen A-3, which had a 0.367 reinforcement index and about twice as much bonded reinforcing steel and tendon as specimen A-2, and Fig. 7(e) shows specimen A-9, which had a 0.55 reinforcement index and about twice as much tendon and about five times as much bonded reinforcing steel as specimen A-2. Because both specimens were over reinforced specimens, of which the reinforcement indices exceeded the limit value ($0.36\beta_1$) that specified in code (ACI Committee 318 2005), they had brittle failure modes-that is, they were collapsed at relatively small curvatures. Nevertheless, the proposed model very accurately described

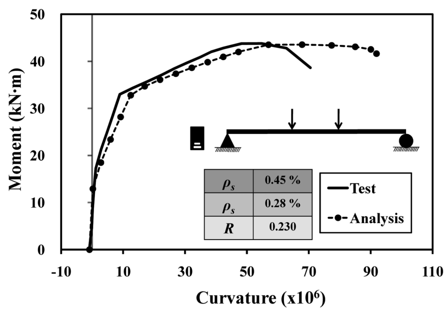

(a) A-2 Specimen

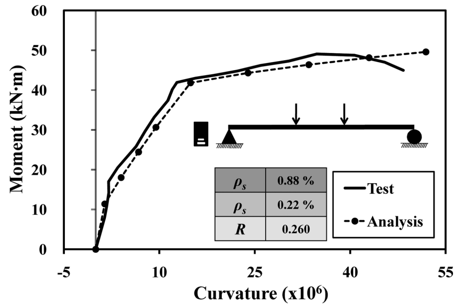

(b) A-5 Specimen

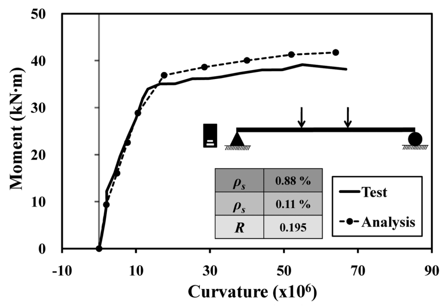

(c) A-7 Specimen

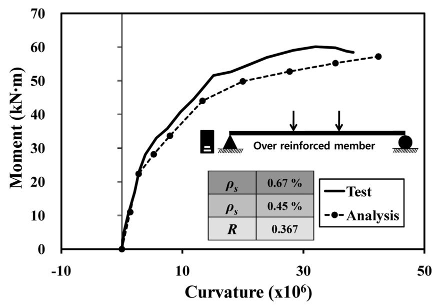

(d) A-3 Specimen

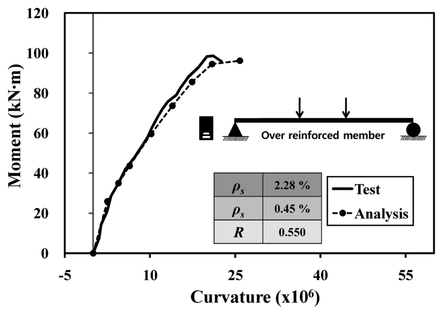

(e) A-9 Specimen

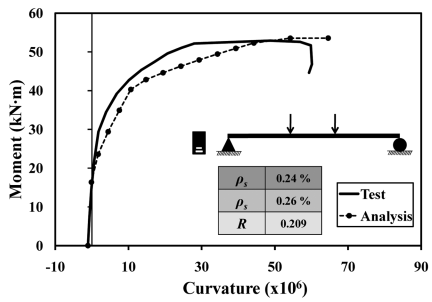

(f) F-1 Specimen

Fig. 7 Comparison of analysis results and test results for specimens under 2-point loading

the flexural behavior of these specimens until their failure, which also implies that the effects of reinforcing steel and tendons on the flexural behavior, even for over-reinforced members, can be well captured by the neutral axis utilized to consider these influences in the proposed model. Therefore, it can be noted that the proposed flexural behavior model very accurately predicts the flexural behavior and strength both under service load state and in the ultimate state even for the over reinforced members that may possibly occur when retrofitting existing members.

Fig. 7(f) shows a two-point loaded member with a 0.24% reinforcing steel ratio and a 0.26% ratio of prestressing tendons, which was somewhat lightly reinforced, compared to the other specimens. The proposed model slightly underestimated the stiffness of specimen after initial cracking, but it provided relatively good estimation of the overall member behavior, especially giving almost identical flexural strength to the test result.

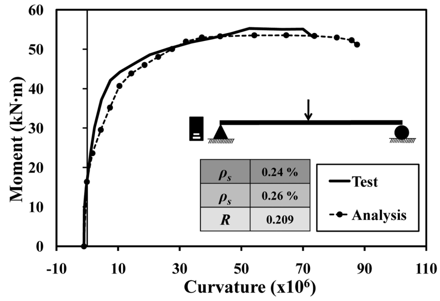

(a) F-2 Specimen

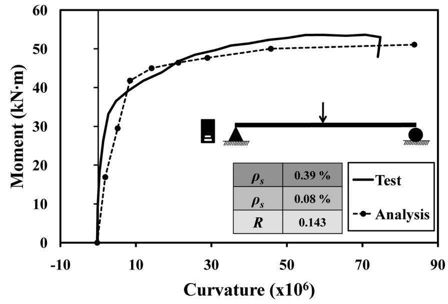

(b) J-1 Specimen

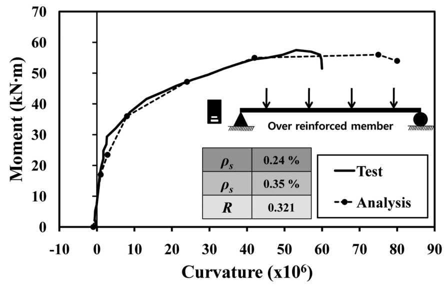

(c) B-2 Specimen

Fig. 8 Comparison of analysis results and test results for specimens under 1-point and 4-point loading

5.2 Members under other loading patterns

Specimen F-2, shown in Fig. 8(a), had the same sectional details as specimen F-1 including the amount of reinforcing steel and prestressing tendons, whereas it was tested under a concentrated loading. The proposed model consistently well predicted not only the initial stiffness but also the flexural behavior after the yield, which means that the consideration on the concentrated loading pattern using the moment area in the proposed model is very reasonable. Fig. 8(b) shows specimen J-1, which was also subjected to a concentrated loading. The reinforcing steel ratio was 0.39% and only one tendon was placed, giving the prestressing tendon ratio only 0.08%, which means that, as indicated by the reinforcement index value of 0.143, this specimen was very lightly reinforced. The

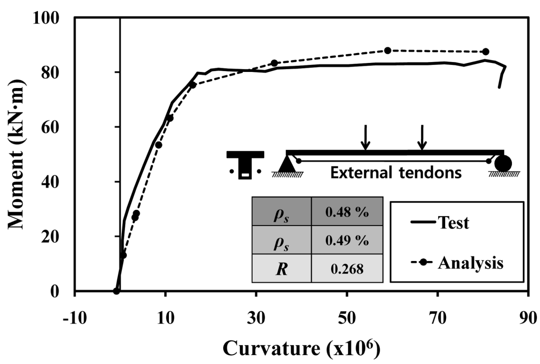

Fig. 9 Comparison of analysis results and test results for specimens with a T-shaped section

proposed model slightly underestimated the initial and post-yield stiffness for this under-reinforced member; however, the ultimate strength and the corresponding curvature were not much different from the test results.

Fig. 8(c) shows specimen B-2, which were subjected to four-point loading that is very close to uniform distributed loading condition. It is an over-reinforced specimen with the reinforcement index exceeding the specified limit value (ACI Committee 318 2005, Korea Concrete Institute 2007). As aforementioned, the proposed model very accurately predicted the flexural behavior and the ultimate strength of the over-reinforced members, and the same observation can be made in the specimen B-2. More importantly, as the loading condition of specimen B-2 was as close as uniformly distributed loading, the accurate estimation of the flexural behavior of specimen B-2 by the proposed model confirms that considering the loading patterns based on the moment area, as used in the proposed model, is also well applicable to the uniform distributed loading case as well.

5.3 Externally post-tensioned members

Specimen T-1, shown in Fig. 9, is an externally post-tensioned member and has a T-shaped section. Based on the width of its upper flange, its reinforcing steel ratio is 0.48% (1.3% based on the web width), and the prestressing tendon ratio is 0.49%. The analysis result shows that the proposed model reasonably well captured the overall flexural behavior of this externally post-tensioned member. Thus, it is considered that the proposed flexural behavior model can be applied without much difficulty to both internally and externally post-tensioned members with various sectional types.

As has been verified above, the proposed flexural behavior model can very accurately predict the flexural behavior and the ultimate strength of UPT members that were either internally or externally post-tensioned, having various ranges of reinforcement index, and subjected to various loading patterns. Therefore, the proposed model is considered to be applicable for the estimation of the flexural behavior and the ultimate strength of post-tensioned members with unbonded tendons.

6. Conclusions

This study aimed to propose a flexural behavior model for post-tensioned members with unbonded tendons and to verify the accuracy and applicability of the proposed model, comparing to the experimental test results available in literature. The following conclusions were obtained from this study.

1. The proposed flexural behavior model very accurately predicted the overall member behavior of post-tensioned members with unbonded tendons, including the initial stiffness, the behavior after cracking and ultimate states.
2. The proposed model very accurately predicts the flexural behavior not only of two-point loading members but also of members with other various loading patterns, such as a concentrated loading and uniformly distributed loading, which supports that the consideration of loading patterns using the moment area is reasonable.
3. The proposed model showed excellent applicability to both internally and externally post-tensioned members.
4. The proposed model can also be used for over-reinforced members, which may possibly occur during retrofit of existing members; and this shows that the neutral axis utilized in the proposed

model well captured the effect of reinforcement ratio on the flexural behavior of UPT members.
5. It was verified that the proposed model is suitable for the estimation of the flexural behavior and the ultimate strength of UPT members.

Acknowledgments

This work was supported by the Korea Research Foundation Grant funded by the Korean Government (MOEHRD, General Research Promotion Fund) (KRF-2010-0003728).

References

ACI Committee 318 (2005), *Building code requirements for structural concrete and commentary (ACI 318M-05)*, American Concrete Institute, Farmington Hills, MI.
ACI Committee 318 (2008), *Building code requirements for structural concrete and commentary (ACI 318M-08)*, American Concrete Institute, Farmington Hills, MI.
Allouche, E.N., Campbell, T.I., Green, M.F. and Soudki, K.A. (1999a), "Tendon stress in continuous unbonded prestressed concrete members - Part 1 parametric study", *PCI J.*, **44**(1), 86-93.
Allouche, E.N., Campbell, T.I., Green, M.F. and Soudki, K.A. (1999b), "Tendon stress in continuous unbonded prestressed concrete members - Part 2: review of literature", *PCI J.*, **44**(1), 86-93.
American Association of State Highway and Transportation Officials (2004), "AASHTO LRFD bridge design specifications", Third edition, AASHTO, Washington, DC.
Au, F.T.K. and Du, J.S. (2004), "Prediction of ultimate stress in unbonded tendons", *Mag. Concrete Res.*, **56**(1), 1-11.
Au, F.T.K., Chan, K.H.E., Kwan, A.K.H. and Du, J.S. (2009), "Flexural ductility of prestressed concrete beams with unbonded tendons", *Comput. Concrete*, **6**(6), 451-472.
Bondy, K.B. (1970), "Realistic reqirements for unbonded post-tensioning tendons", *PCI J.*, **15**(1), 50-59.
Bui, D.K. and Niwa, J. (2006), "Prediction of loading-induced stress in unbonded tendons at ultimate", *Doboku Gakkai Ronbunshu E*, **62**(2), 428-443.
BSI 8110-85 (1985), *Section 4.3.7.3: Structural use of concrete*, British Standards Institution, London.
Campbell, T.I. and Chouinard, K.L. (1991), "Influence of non-prestressed reinforcement on the strength of unbonded partially prestressed concrete member", *ACI Struct. J.*, **88**(5), 546-551.
CAN3-A23.3-M94 (1994), *Design of concrete structure*, Canadian Standard Association, Rexdale, Ontario.
Chakrabarti, P.R. (1995), "Ultimate stress for unbonded post-tensioning tendons in partially prestressed beam", *ACI Struct. J.*, **92**(6), 689-697.
Chen, W.F. (1982), *Plasticity in reinforced concrete*, McGraw-Hill.
Collins, M.P. and Mitchell, D. (1991), *Prestressed concrete structures*, Prentice Hill, Englewood Cliffs, NJ.
DIN 4227 (1980), *Part 6: Prestressed concrete, construction of prestressed concrete member*, German Code, pp. 365.
Du, J.S., Au, F.T.K., Cheung, Y.K. and Kwan, A.K.H. (2008), "Ductility analysis of prestressed concrete beams with unbonded tendons", *Eng. Struct.*, **30**(1), 13-21.
Du, G. and Tao, X. (1985), "Ultimate stress of unbonded tendons in partially prestressed concrete beams", *PCI J.*, **30**(6), 72-91.
Harajli, M.H. (1990), "Effect of span-depth ratio on the ultimate steel stress in unbonded prestressed concrete members", *ACI Struct. J.*, **87**(3), 305-312.
Harajli, M.H. (2006), "On the stress in unbonded tendon at ultimate: critical assessment and proposed change", *ACI Struct. J.*, **103**(6), 803-812.
Harajli, M.H. and Kanj, M.Y. (1991), "Ultimate flexural strength of concrete members prestressed with unbonded tendons", *ACI Struct. J.*, **88**(6), 663-673.
Harajli, M.H. and Kanj, M.Y. (1997), "Service load behavior of concrete members prestressed with unbonded

tendons", *J. Struct. Eng.-ASCE*, **94**(1), 2569-2589.

Harajli, M.H., Khairallah, N. and Nasif, H. (1999), "Externally prestressed members: evaluation of sencond-order effect", *J. Struct. Eng.-ASCE*, **125**(10), 1151-1161.

Janney, J.R., Hognestad, E. and Mchenry, D. (1956), "Ultimate flexural strength of prestressed and conventionally reinforced concrete beam", *ACI Struct. J.*, **52**(2), 601-620.

KCI-M-07 (2007), *Design specifications for concrete structures*, Korea Concrete Institute.

Lee, S.H., Yeo, U.S., Shin, K.J. and Kim, W.J. (2010), "Analytical study on strengthening effect of RC beams strengthened with high-tension steel rod", *2010 Struct. Congr.-ASCE*, 3590-3601.

Lim, J.H., Moon, J.H. and Lee, L.H. (1999), "Experimental examination of influential variables on unbonded tendon stresses", *J. Korean Concrete Inst.*, **11**(1), 209-219.

Lee, D.H. and Kim, K.S. (2011), "Flexural strength of prestressed concrete members with unbonded tendons", *Struct. Eng. Mech.*, **38**(5), 675-696.

Lee, L.H., Moon, J.H. and Lim, J.H. (1999), "Proposed methodology for computing of unbonded tendon stress at flexural failure", *ACI Struct. J.*, **96**(6), 1040-1048.

Mattock, A.H. (1979), "Flexural strength of prestressed concrete sections by programable calculator", *PCI J.*, **24**(1), 32-54.

MacGregor, R.J.G., Kreger, M.E. and Breen, J.E. (1989), "Strength and ductility of three span externally post-tensioned segmental box girder bridge model", *Research Report*, No. 365-3F, Center for Transportation Research, The University of Texas, Austin, Texas.

Mojtahedi, S. and Gamble, W.L. (1978), "Ultimate steel stresses in unbonded prestressed concrete", *J. Struct. Div.*, **104**(7), 1159-1165.

Moon, J.H., Lim, J.H. and Lee, C.G. (2002), "Relation of deflection of prestressed concrete members to unbonbded tendon stress and effect of various parameters", *J. Korean Concrete Inst.*, **14**(2), 171-179.

Naaman, A.E. and Alkhairi, F.M. (1991a), "Stress at ultimate in unbonded post tensionning tendons - Part 1: evaluation of the state-of-the-art", *ACI Struct. J.*, **88**(5), 641-651.

Naaman, A.E. and Alkhairi, F.M. (1991b), "Stress at ultimate in unbonded post tensionning tendons - Part 2: proposed methodology", *ACI Struct. J.,* **88**(6), 693-692.

Ng, C.K. (2003), "Tendon stress and flexural strength of externally prestressed beams", *ACI Struct. J.*, **100**(5), 644-653.

NEN 3880 (1984), *Part H: Regulations for concrete*, Dutch Code, Section 503.1.3.

Ozkul, O., Nasif, H.H. and Malhas, F. (2005), *Deflection prediction and cracking of beams prestressed with unbonded tendons*, Serviceability of Concrete: A Symposium Honoring Dr. E.G. Nawy, SP-225, American Concrete, Institute, Farmington Hills, MI, 93-118.

Ozkul, O., Nassif, H., Tanchan, P. and Harajli, M.H. (2008), "Rational approach for predicting stress in beams with unbonded tendons", *ACI Struct. J.*, **105**(3), 338-347.

Roberts-Wollmann, C.L., Kreger, M.E., Rogosky, D.M. and Breen, J.E. (2005), "Stress in external tendons at ultimate", *ACI Struct. J.*, **102**(2), 206-213.

Sivaleepunth, C., Niwa, J., Bui, D.K., Tamura, S. and Hamada, Y. (2006), "Prediction of tendon stress and flexural strength of externally prestressed concrete beams", *Doboku Gakkai Ronbunshu E*, **62**(1), 260-273.

Tam, A. and Pannell, F.N. (1976), "The ultimate moment resistance of unbonded partially prestressed reinforced concrete", *Mag. Concrete Res.*, **28**(97), 203-208.

Tan, K.H. and Tjandra, R.A. (2007), "Strengthening of RC continuous beams by external prestressing", *J. Struct. Eng.-ASCE*, **133**(2), 195-204.

Warwaruk, J., Sozen, M.A. and Siess, C.P. (1962), *Investigation of prestressed concrete for highway bridges, Part.: strength and behavior in flexure of prestressed beam*, Bulletin No. 464, Engineering Experiment Station, University of Illinois, Urbana, Ill.

Zhou, W. and Zheng, W.Z. (2010), "Experimental research on plastic design method and moment redistribution in continuous concrete beams prestressed with unbonded tendons", *Mag. Concrete Res.*, **62**(1), 51-64.

CC

Notations

α = coefficient of moment distribution shape
α_1 = stress block factor
β_1 = factor of equivalent rectangular compressive stress block depth to neutral axis depth
k = ratio of maximum moment region to beam length
f_c = stress of concrete
f_s = stress of reinforcing bar
f_c' = specified compressive strength of concrete
f_r = modulus of ruptre
f_{ps} = stress of prestressed tendon
f_{pe} = effective prestress in prestressing steel
f_{pu} = ultimate strength of prestressing steel
f_{py} = yield stress of prestressing steel
f_y = yield stress of reinforcing steel
E_c = modulus of elasticity of concrete
E_s = modulus of elasticity of reinforcement and structural steel
ε_c = strain of concrete
ε_s = strain of tensile reinforcement
ε_s' = strain of compression reinforcement
ε_y = yield strain of reinforcement
ε_{cr} = cracking strain
ε_x = strain at arbitrary location from extreme top fiber
ε_t = strain at extrem top fiber
ε_b = strain at extrem bottom fiber
ε_{pe} = effective prestrain in prestressing steel $= f_{pe}/E_{ps}$
$\Delta\varepsilon_{c,ps}$ = additional strain of concrete at tendon height
ε_{ps} = strain in prestressing steel at ultimate state
ϕ = beam curvature
ϕ_m = beam curvature at maximum moment
c_x = depth of neutral axis
c_m = depth of neutral axis at ultimate
c_y = neutral axis depth assuming $f_{ps} = f_{py}$
y_b = distance from centroid of section to extrem bottom fiber
y = distance from extrem compression fiber to arbitrary location along the depth
$\bar{y}$ = distance from neutral axis to centroid of equivlent stress block
b_w = flange width
d = distance from extrem compression fiber to centroid of tension reinforcement
d' = distance from extrem compression fiber to centroid of compression reinforcement
d_p = distance from extrem compression fiber to centroid of prestressing steel
h = height of section
I_g = moment of inertia
h = height of section
L_m = constant moment region
L_p = equivalent plastic hinge length

A_{ps} = area of unbonded prestressing steel
A_s = area of ordinary tension steel
A_s' = area of compression steel
ρ_p = ratio of prestressed steel = A_{ps}/b_p
ρ_s = ratio of ordinary bonded steel = A_s/b_d
ω_s = tension reinforcing index
ω_s' = compression reinforcing index
ω_p = prestressing steel index
R = reinforcing index
P_u = ultimate external load
M_{cr} = cracking moment
M_n = ultimate moment capacity of UPT beam